PCCP

Accepted Manuscript

ROYAL SOCIETY OF CHEMISTRY

www.rsc.org/pccp

Drastic Alteration of Diffusioosmosis due to Steric Effects

Vahid Hoshyargar [a], Seyed Nezameddin Ashrafizadeh [a], Arman Sadeghi [b,1]

[a] *Research Lab for Advanced Separation Processes, Department of Chemical Engineering, Iran University of Science and Technology, Narmak, Tehran 16846-13114, Iran*

[b] *Department of Mechanical Engineering, University of Kurdistan, Sanandaj 66177-15175, Iran*

ABSTRACT

The inclusion of the ionic size (steric) effects into the steady and locally developed diffusioosmotic flow inside a uniformly charged slit microchannel through a theoretical analysis is the subject of this study. The results indicate essential quantitative and qualitative distinctions between the steric effects on classical electrokinetic phenomena like electroosmosis and on diffusioosmosis. For example, although the steric effect on electroosmotic flow is always unfavorable, it may have a positive influence on diffusioosmosis and even double the mean velocity under certain conditions. Moreover, finite ionic sizes can even change the flow direction with a tendency to increase the chance of flow toward higher concentration. Another interesting finding is that, unlike electroosmosis, the steric effects on diffusioosmotic flow do not vanish even when the EDL is very thin. The main quantitative difference between the ionic size effects on diffusioosmosis and the other electrokinetic phenomena is the critical zeta potential above which these effects become important which is here found to be only about several tens of millivolts. The more sensitivity of diffusioosmosis to the steric effects and also the above-mentioned surprisingly different trends are attributed to the induced electric field which may drastically get influenced by the steric factor.

Keywords: Diffusioosmotic flow; Slit microchannel; Steric effects

[1] Corresponding author
E-mail addresses: hoshyargar@iust.ac.ir (V. Hoshyargar), ashrafi@iust.ac.ir (S.N. Ashrafizadeh), a.sadeghi@eng.uok.ac.ir (A. Sadeghi)

1. INTRODUCTION

Microfluidics has been a growing research field through the past two decades because of its unique specifications which have resulted in its wide applications in different microdevices such as the clinical diagnosis instruments called lab-on-a-chip (LOC). High test speed, low sample and/or reagent consumption, and executing multiple tests simultaneously are just some of the many advantages of these devices. The main functions being performed in LOCs including transport, mixing, and separation of samples are usually carried out by making use of the electrokinetic phenomena[1-6]. The main reason the electrokinetic-based mechanisms are favored over the classical instruments is that they usually do not have any moving parts which increases their reliability and drastically simplifies the production process. Moreover, they are easily incorporated into the whole design and the operating parameters are fully under control with a much smaller response time.

The classical electrokinetic phenomena including electroosmosis, streaming potential, electrophoresis, and sedimentation potential are usually classified by the criterion that whether the electric field is external or is induced by a mechanically-driven motion. When an ionic concentration gradient is served as the driving force, a fluid flow named diffusioosmosis and a particle motion termed diffusiophoresis are achieved[7-10]. The diffusioosmotic flow, which is the subject of the present study, is created when a tangential concentration gradient of an electrolyte next to a charged wall spontaneously sets up both an induced electric field (IEF) and an osmotic pressure gradient. The electric field upon acting on the net electric charge within the electric double layer (EDL) near the wall creates a net fluid flow which together with that created by the osmotic pressure gradient constitutes a diffusioosmotic flow. It deserves mentioning that although diffusioosmosis (DO) occurs in many practical applications, nonetheless, for cases involving other driving forces (*e.g.* electric field or pressure gradient) its effects are usually negligible because of having very low flow rates.

Although, in comparison with the other electrokinetic phenomena, diffusioosmosis has received less attention in the literature[7, 8, 11-26] but the highlight of DO is attributed to flow actuation under no external electric field or pressure gradient while both are intrinsically created[27, 28]. Also the concentration-dependent velocity of DOF may have applications in self-regulated drug delivery systems where the release rate of the drug can be regulated as a function of the physiological change in pH[29]. Besides, DO could be important in LOC devices or biosensors wherein it is capable of intensifying the current recognition which gives rise to enhancing the performance of moving charged particles[30]. Although DO is not as good as electroosmosis (EO) in flow control, but where there is a need for continuous, long lasting, easier fabrication, and restriction of no external driving force, it can be a proper option.

Whereas the main aspects of DO for both Newtonian[7, 8, 11-22, 31] and non-Newtonian[23-26] behaviors and at low[12, 14, 15, 17, 21, 25, 32] and high[7, 8, 11, 13, 16, 18-20, 22, 23, 26] surface potentials have been totally explored, all of our knowledge is based on considering the ions to be effective point charges. The ions, however, are of finite sizes and such an assumption may lead to significant errors when either the channel characteristic length is very small or the ionic concentration is high, especially at large surface potentials for which there will be a huge condensation of ions near the wall[33-46]. The importance of the ionic size (steric) effects is determined by the steric factor ν which is the mean volume fraction of each ion in the bulk and is therefore given as $\nu = a^3 n^\infty$. In this relationship, a denotes the effective ionic size and n^∞ is the ionic concentration at neutral conditions. The fact that the effective ionic size is considered instead of common radius is due to gyration radius made by hydration of ions surrounded by water molecules that could extend a up to several nanometers[34]. Such high values

of a for ionic concentrations of about several tens of moles per cubic meter may result in the steric factors of the order 0.1 which is believed to be high enough for the steric effects to show up at moderate zeta potentials.

The aim of the present work is to theoretically analyze the ionic size effects on diffusioosmotic flow invoking the Bikerman's model[47]. Along this line, a slit-like geometry is chosen for a better tractability of the problem. The smallness of the ionic concentration gradient, the validity of a locally developed flow, as well as the uniformity and constancy of the surface potential are the limiting assumptions considered. The results show up to 2 orders of magnitude increase in IEF along with a doubled mean velocity just for a low steric factor of 0.05, indicating that considering steric effects is inevitable in many practical situations.

2. MATHEMATICAL FORMULATION

Diffusioosmotic flow in a slit microchannel of height $2H$ is theoretically being investigated by taking the ionic size effects into account. The schematic of the physical problem including the direction of decrease in the number concentration in the bulk $n^{\infty}(z)$ and the coordinate system is given in Fig. 1. We assume that the flow is steady and locally developed and the liquid is a symmetric electrolyte of valence $\mathbb{z}$. It is further assumed that the zeta potential is constant and uniform. Finally, it is supposed that the ionic concentration gradient ∇n^{∞} is negligible as compared with n^{∞} for the axial variations of the electrostatic potential and ionic concentration to remain negligible.

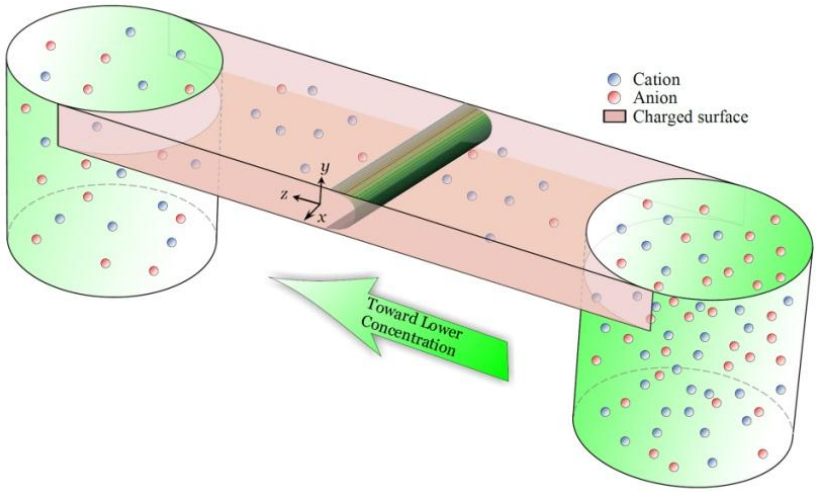

Fig. 1. Schematic representation of the slit microchannel including the direction of decrease in the number concentration in the bulk and the coordinate system.

2.1. Electrical Potential Distribution

One of the main parts of any analysis of the electrokinetic phenomena is to evaluate the electrical potential distribution within the domain. Of the two components of the electrical potential in diffusioosmosis, that is the EDL potential and that associated with the induced electric field, only the former is to be dealt with in this section. The electric potential within dielectric materials is described by the Poisson equation which for our case reduces to

$$\frac{\mathrm{d}^2\psi}{\mathrm{d}y^2} = -\frac{\rho_e}{\varepsilon} \tag{1}$$

where ψ stands for the EDL potential, ε represents the fluid permittivity, and $\rho_e = \mathbb{z}e(n_+ - n_-)$ is the net electric charge density with e being the proton charge. It can be shown that, when the ionic size is taken into account, the ionic concentration for a two component solution is given by the following modified form of the Boltzmann distribution[40]

$$n_\pm = \frac{n^\infty \mathrm{e}^{\left(\mp\frac{\mathbb{z}e\psi}{k_BT}\right)}}{1 + 4\nu \sinh^2\left(\frac{\mathbb{z}e\psi}{2k_BT}\right)} \tag{2}$$

Here, k_B is the Boltzmann constant and T denotes the absolute temperature. Substituting Eq. (2) into the charge density relationship and using it in the Poisson equation, one comes up with the modified Poisson-Boltzmann equation, also known as Poisson-Bikerman equation, given as

$$\frac{\mathrm{d}^2\psi}{\mathrm{d}y^2} = \frac{2n^\infty \mathbb{z}e}{\varepsilon} \frac{\sinh\left(\frac{\mathbb{z}e\psi}{k_BT}\right)}{1 + 4\nu \sinh^2\left(\frac{\mathbb{z}e\psi}{2k_BT}\right)} \tag{3}$$

which is reduced to the classical Poisson-Boltzmann equation for the conditions under which the ionic size effects are negligible, that is when $\nu = 0$. Unlike the classical Poisson-Boltzmann equation, Eq. (3) does not predict unrealistically large ion densities adjacent to highly charged surfaces; instead, at a certain critical zeta potential a maximum density is reached[36]. Utilizing the Debye length, given as $\lambda_D = (2n^\infty e^2 \mathbb{z}^2/\varepsilon k_B T)^{-1/2}$, and introducing the dimensionless parameters $\psi^* = \mathbb{z}e\psi/k_BT$, $y^* = y/H$, and $\mathrm{K} = H/\lambda_D$, the dimensionless Poisson-Bikerman equation reads

$$\frac{\mathrm{d}^2\psi^*}{\mathrm{d}y^{*2}} = \frac{\mathrm{K}^2 \sinh\psi^*}{1 + 4\nu \sinh^2(\psi^*/2)} \tag{4}$$

Writing $\mathrm{d}^2\psi^*/\mathrm{d}y^{*2}$ as $(\mathrm{d}\psi^*/\mathrm{d}y^*)[\mathrm{d}(\mathrm{d}\psi^*/\mathrm{d}y^*)/\mathrm{d}\psi^*]$ and multiplying both sides of Eq. (4) by $\mathrm{d}\psi^*$, it may be integrated across the channel height regarding $\mathrm{d}\psi^*/\mathrm{d}y^* = 0$ at centerline where $\psi^* = \psi_c^*$ to yield

$$\frac{\mathrm{d}\psi^*}{\mathrm{d}y^*} = \pm\sqrt{\frac{\mathrm{K}^2}{\nu}\ln\left(\frac{1 - 2\nu + 2\nu\ \cosh\psi^*}{1 - 2\nu + 2\nu\ \cosh\psi_c^*}\right)} \tag{5}$$

Taking the positive sign in Eq. (5) for the upper half of the channel, a one more integration with the consideration of the fact that the electrical potential at the wall is the so-called zeta potential ζ provides

$$y^* = 1 - \int_{\psi^*}^{\zeta^*} \frac{\mathrm{d}\psi^*}{\sqrt{\frac{\mathrm{K}^2}{\nu}\ln\left(\frac{1 - 2\nu + 2\nu\ \cosh\psi^*}{1 - 2\nu + 2\nu\ \cosh\psi_c^*}\right)}} \tag{6}$$

Hence we have an implicit relationship for the electrical potential in the form $y^* = f(\psi^*)$. The main difficulty in using Eq. (6) is the determination of ψ_c^* which is not known a priori. Our calculations show that this parameter may be set to zero for $5 \leq \mathrm{K}$

without incurring any significant error. For smaller values of the Debye-Hückel parameter K, the shooting method may be invoked to obtain ψ_c^* using the criterion that the corresponding value of y^* be sufficiently close to zero.

2.2. Induced Electric Field (IEF) Distribution

The concentration gradient of the ions forces them to travel along the channel. Since dissimilar species are of generally different diffusivities, a larger number of the ionic type having a higher diffusion coefficient will present at the region of lower concentration. This phenomenon, which sets up an electrical potential difference between the two channel ends, may occur even when the ionic diffusivities are similar, due to the fact that there is an excess of counterions over coions within EDL. The non-uniformity of the ionic concentration in the axial direction also gives rise to the so-called osmotic pressure gradient that creates a fluid flow termed chemiosmosis. This type of flow coupled with the electroosmotic flow created by the induced electric filed upon acting on the net electric charge within EDL results in a diffusioosmotic flow. The determination of the induced electric field is crucial for the electroosmotic part of the flow to be evaluated. Following the literature, we determine the electric field by equating the total axial ionic flux in the axial direction to zero. In the presence of the steric effects, the ionic flux vector, **J**, is given by the following modified form of the Nernst-Planck equation[48, 49]

$$\mathbf{J}_{\pm} = -D_{\pm}\left[\nabla n_{\pm} + \frac{\nu n_{\pm}\sum_k \nabla n_k}{n^{\infty} - \nu\sum_k n_k} \pm \frac{\mathbb{z}en_{\pm}}{k_B T}(\nabla\psi - \mathbf{E})\right] + n_{\pm}\mathbf{u} \tag{7}$$

where **u** represents the velocity vector, $D_{\pm}$ is the diffusion coefficient of the cations/anions, and **E** represents the IEF that acts in z-direction only. Equating $J_{+,z}$ and $J_{-,z}$, we get

$$\begin{aligned} -D_+\left[\frac{\nabla n^{\infty}}{n^{\infty}} n_+\left(1 + \frac{\nu\sum_k n_k}{n^{\infty} - \nu\sum_k n_k}\right) - \frac{\mathbb{z}en_+}{k_B T}E_z\right] + n_+ u_z \\ = -D_-\left[\frac{\nabla n^{\infty}}{n^{\infty}} n_-\left(1 + \frac{\nu\sum_k n_k}{n^{\infty} - \nu\sum_k n_k}\right) + \frac{\mathbb{z}en_-}{k_B T}E_z\right] + n_- u_z \end{aligned} \tag{8}$$

wherein $\nabla_z n_{\pm}$ has been replaced with $\nabla n^{\infty} n_{\pm}/n^{\infty}$ by making use of Eq. (2). Solving for E_z yields

$$E_z = \frac{k_B T}{\mathbb{z}e}\frac{\nabla n^{\infty}}{n^{\infty}}\left[\frac{D_+ n_+ - D_- n_-}{D_+ n_+ + D_- n_-}\left(1 + \frac{\nu\sum_k n_k}{n^{\infty} - \nu\sum_k n_k}\right) + \frac{n^{\infty}}{\nabla n^{\infty}}\frac{u_z(n_- - n_+)}{D_+ n_+ + D_- n_-}\right] \tag{9}$$

that is reduced to the following form by utilizing dimensionless parameters

$$E_z = \frac{k_B T}{\mathbb{z}e}\frac{\nabla n^{\infty}}{n^{\infty}}\left\{\frac{(1+\beta)\mathrm{e}^{-\psi^*} - (1-\beta)\mathrm{e}^{\psi^*}}{(1+\beta)\mathrm{e}^{-\psi^*} + (1-\beta)\mathrm{e}^{\psi^*}}\left[\frac{1 + 4\nu\sinh^2(\psi^*/2)}{1 - 2\nu}\right] + \frac{\mathrm{sgn}(\nabla n^{\infty})Pe\sinh\psi^*}{(1+\beta)\mathrm{e}^{-\psi^*} + (1-\beta)\mathrm{e}^{\psi^*}}u^*\right\} \tag{10}$$

in which $\beta = (D_+ - D_-)/(D_+ + D_-)$ is the dimensionless diffusivity difference and $Pe = 4n^{\infty}U/(D_+ + D_-)|\nabla n^{\infty}|$ represents the Peclet number with U being the characteristic velocity of DOF, given as

$$U = \frac{2k_B T\lambda_D^2}{\mu}|\nabla n^{\infty}| \tag{11}$$

Besides, $\mathrm{sgn}(\nabla n^{\infty}) = |\nabla n^{\infty}|/\nabla n^{\infty}$ and $u^{*} = u_z/U$ denotes the dimensionless axial velocity. It is worth noting that Eq. (10) is reduced to the expression of IEF given by Ma and Keh[18] for DOF in a fine capillary slit by setting $\nu = 0$. The electric field far away from the wall where the electrical potential approaches zero becomes

$$E^{\infty} = \frac{k_B T \nabla n^{\infty}}{\mathbb{z} e n^{\infty}} \left(\frac{\beta}{1 - 2\nu} \right) \tag{12}$$

2.3. Velocity Distribution

The physical principle governing the velocity distribution of surface driven phenomena is the momentum conservation equation with a body force vector **F** that, for a Newtonian behavior, is written as

$$\rho \frac{\mathrm{D}\mathbf{u}}{\mathrm{D}t} = -\nabla p + \mu \nabla^2 \mathbf{u} + \mathbf{F} \tag{13}$$

where ρ represents the fluid density and p is the pressure. For the present case, $\mathbf{F} = \rho_e(\mathbf{E} - \nabla\psi)$ and therefore acts in both y and z directions. The equation of continuity suggests a velocity vector of the form $\mathbf{u} = [\,0, u_z(y)]$ for a fully developed incompressible flow; on the other hand, for a steady fully developed flow $\mathrm{D}\mathbf{u}/\mathrm{D}t = 0$. Under this circumstance, the following equations are reached

$$-\frac{\partial p}{\partial y} - \rho_e \frac{\mathrm{d}\psi}{\mathrm{d}y} = 0 \tag{14a}$$

$$-\frac{\partial p}{\partial z} + \mu \frac{\mathrm{d}^2 u_z}{\mathrm{d}y^2} + \rho_e E_z = 0 \tag{14b}$$

Multiplying both sides of Eq. (14a) by $\mathrm{d}y$ and integrating with the consideration of the associated boundary conditions, one will have

$$p = p^{\infty} + \frac{n^{\infty} k_B T}{\nu} \ln \left[\frac{2\nu \cosh\left(\frac{\mathbb{z} e \psi}{k_B T}\right) - 2\nu + 1}{2\nu \cosh\left(\frac{\mathbb{z} e \psi_c}{k_B T}\right) - 2\nu + 1} \right] \tag{15}$$

where $p^{\infty}(z)$ is the centerline pressure. Having the pressure distribution in hand, one can simply derive an expression for the axial pressure gradient required for solving Eq. (14b). This is done by assuming a negligible ∇p^{∞} as a consequence of no applied pressure force, leading to the following z-momentum equation

$$\mu \frac{\mathrm{d}^2 u_z}{\mathrm{d}y^2} = \frac{k_B T \nabla n^{\infty}}{\nu} \ln \left[\frac{2\nu \cosh\left(\frac{\mathbb{z} e \psi}{k_B T}\right) - 2\nu + 1}{2\nu \cosh\left(\frac{\mathbb{z} e \psi_c}{k_B T}\right) - 2\nu + 1} \right] + 2\mathbb{z} e n^{\infty} E_z \frac{\sinh\left(\frac{\mathbb{z} e \psi}{k_B T}\right)}{1 + 4\nu \sinh^2\left(\frac{\mathbb{z} e \psi}{2 k_B T}\right)} \tag{16}$$

Integrating the dimensionless form of Eq. (16) with respect to y^{*} from centerline to an arbitrary point with the consideration of the symmetry conditions and integrating the resultant equation again from the wall to an arbitrary place subject to the no slip conditions, one can obtain the velocity field as

$$u^* = \int_1^{y^*} \int_0^{y^*} \mathrm{K}^2 \mathrm{sgn}(\nabla n^\infty) \left[\frac{1}{2\nu} \ln \left(\frac{2\nu \cosh \psi^* - 2\nu + 1}{2\nu \cosh \psi_c^* - 2\nu + 1} \right) + \frac{\beta \sinh \psi^* E^*}{1 + 4\nu \sinh^2(\psi^*/2)} \right] \mathrm{d}y^* \mathrm{d}y^* \quad (17)$$

wherein the dimensionless electric field is $E^* = E_z / E_{\nu=0}^{\infty}$.

Before proceeding further, we skim through the domain of operating conditions in which DOF is important in practical situations. Evidently, diffusioosmosis is the only important phenomenon wherever solely an ionic concentration gradient is present. If DOF is accompanied by other driving forces, its importance is determined by checking the ratio of DOF characteristic velocity to the velocity scale of the other external driving force. As it is usually the case, when the external force is either of an electric field or a pressure gradient, the DOF velocity given by Eq. (11) should be compared with the Helmholtz-Smoluchowski electroosmotic velocity $-\varepsilon\zeta E_z/\mu$ and the pressure-driven velocity scale, given by $-H^2\nabla p^\infty/2\mu$. Accordingly, when ($|\varepsilon\zeta E_z|$ or $|H^2\nabla p^\infty/2|$) $\geq 20 k_B T \lambda_D^2 |\nabla n^\infty|$ DOF may be ignored whereas it is the only phenomenon of interest for cases in which ($|\varepsilon\zeta E_z|$ or $|H^2\nabla p^\infty/2|$) $\leq k_B T \lambda_D^2 |\nabla n^\infty|/5$. When ($|\varepsilon\zeta E_z|$ or $|H^2\nabla p^\infty/2|$)$\sim 2 k_B T \lambda_D^2 |\nabla n^\infty|$ a thorough analysis should be performed by taking all effects into account.

3. RESULTS AND DISCUSSION

A quick glance at Eqs. (10) and (17) reveals that the electric and velocity fields are strongly coupled and hence should be obtained simultaneously. Method of solution starts by calculating the electric field utilizing Eq. (10) assuming a zero velocity and using it in Eq. (17) to evaluate the velocity distribution. The predicted velocity values are then used to estimate a new electric field. The procedure is going on until the relative difference between the results of two successive steps reaches a value less than a certain tolerance. It is worth mentioning that since the procedure presented is based on a non-zero ν for which no data is available in the literature, our results were validated utilizing those reported by Ma and Keh [18] for DOF with no steric effects by limiting the steric factor to zero. The comparison, which is omitted here for brevity, revealed a complete agreement between the results conforming a common condition of $Pe = 0$.

The presentation of results starts by illustrating the steric effects on the mean velocity in dimensionless form given as $u_m^* = \int_0^1 u^* \mathrm{d}y^*$ in Fig. 2. The mean velocity is the most valuable parameter to a LOC designer. Comparing the two parts of Fig. 2 reveals that the steric effects are more pronounced at high surface potentials, in agreement with our previous deductions. The alteration due to the ionic size effect is absolutely vital at high ζ^* since, unlike low zeta potentials, it not only affects the magnitude but also can change the flow direction. It is observed that the mean velocity generally increases in magnitude when taking the ionic size into account, in sharp contrast to EO[45]. Although the physical interpretation of the variations is generally very difficult because of the complicated nature of DO, we try to do this by considering the special case of $\beta = -1$ for which the diffusivity of the positive ions is negligibly small. For this case, there will be an accumulation of the negative ions at the region of lower concentration, establishing a positive electric field which creates a negative velocity upon acting on mostly negative ions within EDL, as justified by the figure. When the ionic size is accounted for, the number of the ions in EDL is reduced leading to a smaller pressure gradient which in this case is unfavorable. This is the first reason of getting higher flow rates. On the other hand, the reduction of the ions

within EDL could result in a lower body force if the induced electric field was remained unchanged, as is the case for EO[45]. Nonetheless, in case of DO the electric field may be amplified since, according to Eq. (7), the ionic flux in the axial direction in the presence of the steric effects is higher under the same conditions. The significantly higher value of the electric field that can overcome the reduction in the charge density is the second and main reason of the mean velocity being larger in the presence of steric effects.

The more intense steric impacts for negative values of β may be attributed to the fact that, when the ions are assumed to be of finite volume, the ratio of the counter ions to the coions increases near the wall to neutralize the unchanged surface charge[36]. This slightly increases the electric field when β is negative; however, the opposite is true when $D_- < D_+$ since it gives rise to a smaller number of cations at the channel end where the positive pole of IEF locates. Moreover, the pressure gradient, which is reduced by the steric effects, is mostly in favor of flow for this case. Another interesting point taken from Fig. 2 is that, unlike EO, the asymptotic values of velocity at thin EDL limit with and without steric effects differ significantly. The reason is that even when the double layer effects on IEF are small, it is amplified by the higher ionic fluxes in the bulk when the ionic size is included.

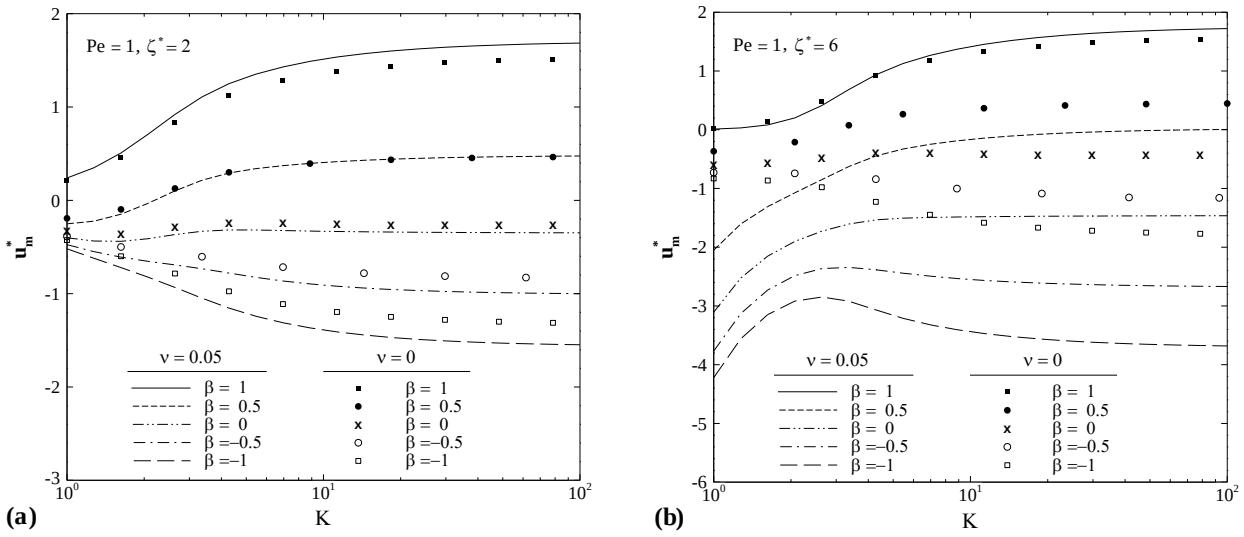

Fig. 2. Mean velocity vs. K at different β and ν for a) $\zeta^* = 2$ and b) $\zeta^* = 6$.

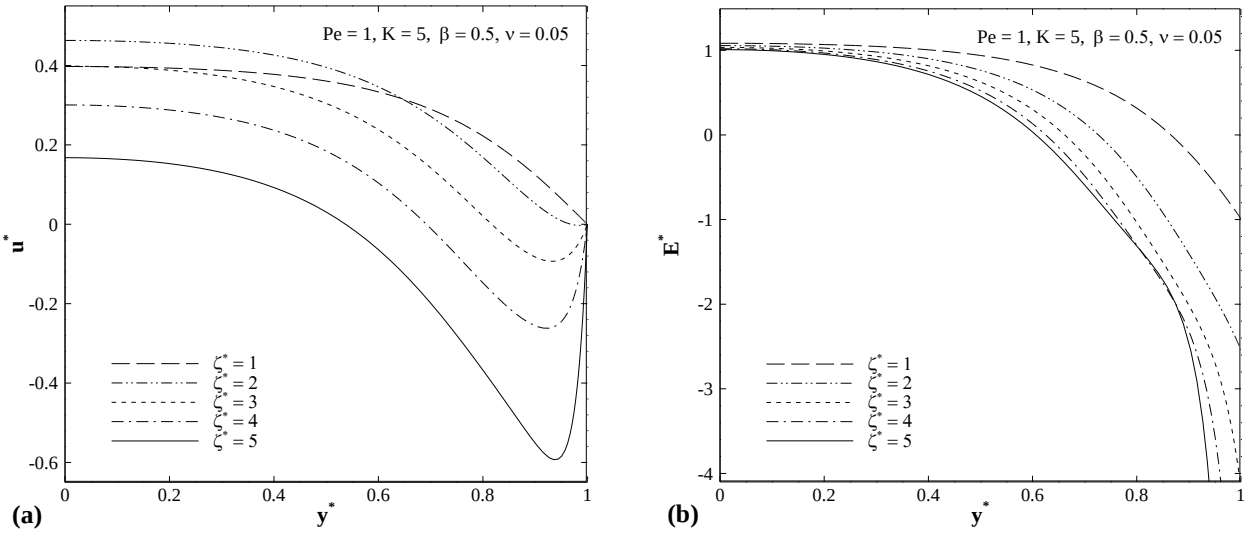

Fig. 3. Distributions of (a) velocity and (b) induced electric field in normalized form at different values of ζ^*.

The influences of the zeta potential on the velocity profile for $\beta = 0.5$ are studied through Fig. 3a. The corresponding electric field distributions are also shown in part b of the figure. It is noted that for the case the ions cannot be considered as point charges quite different patterns may be achieved for the velocity by varying the surface potential. Specifically, an irregular velocity overshoot is seen adjacent to the wall for high zeta potentials. At small zeta potentials such as $\zeta^* = 1$, the electric field is mainly negative (note that $E_{\nu=0}^{\infty}$ used for normalization of IEF is negative itself), because of the excess of cations over anions having a smaller diffusivity at the channel end, producing a positive velocity. By increasing the surface charge, the number of mostly anions located within the double layer is increased. In addition, as mentioned previously, the ratio of anions to cations will be higher due to the more intense steric effects. Accordingly, we may anticipate more accumulation of the negative ions at the channel end, especially near the wall, resulting in a positive electric field therein, as observed in the figure. The mentioned change in IEF gives rise to a reverse flow near the wall since the net electric charge is negative close to the channel surface. A careful inspection of the velocity profile for $\zeta^* = 5$ reveals that unlike EO the increase of the surface potential may not be a good idea for getting higher flow rates when the ionic size effects are included at the time $\beta > 0$.

Since most of the body force is produced adjacent to the wall, the value of the electric field at the wall, E_w, has a significant impact on the velocity profile. Fig. 4 illustrates the functionality of the normalized form of this parameter on the zeta potential at various steric factors. The interesting point with reference to the ionic size consideration is that whereas the premise of point charge ions looks reasonable when either $\nu \leq 10^{-3}$ or $\zeta^* \leq 1$ ($\zeta \leq 25$ mV) it could lead to dramatic errors at high surface charges for which the inclusion of the steric effects may lead to even 2 orders of magnitude larger electric fields. As the effective ionic size increases, the chance of presence within EDL is decreased for cations since the same number of anions are needed to neutralize the positively charged surface; accordingly, the anions gradually form a packed-shaped layer contiguous to the wall that leads to more accumulation of negative charge at the channel end, thereby amplifying the electric field, as is clear in Fig. 4.

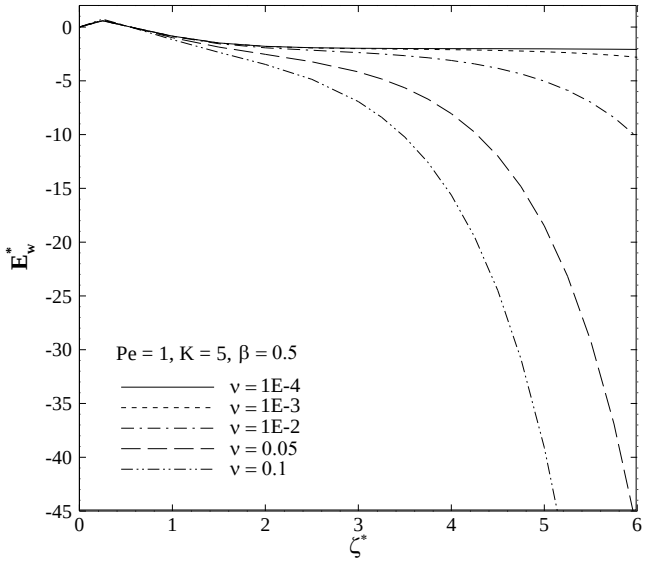

Fig. 4. Induces electric field at the wall vs. ζ^* at different steric factors.

A better demonstration of how the steric factor affects DO is presented in Fig. 5 which depicts the centerline velocity versus ν. It is totally interesting that serious alterations are started at about $\nu = 3 \times 10^{-2}$, a value that is very low to cause variations in EO[40, 43, 45]. It can be seen that, in case of positively charged surface, such a phenomenon gets bolder as the diffusivity of the anions increases. The opposite should be the case for negatively charged wall since DO always comes with a symmetrical response with respect to ζ^* and β.

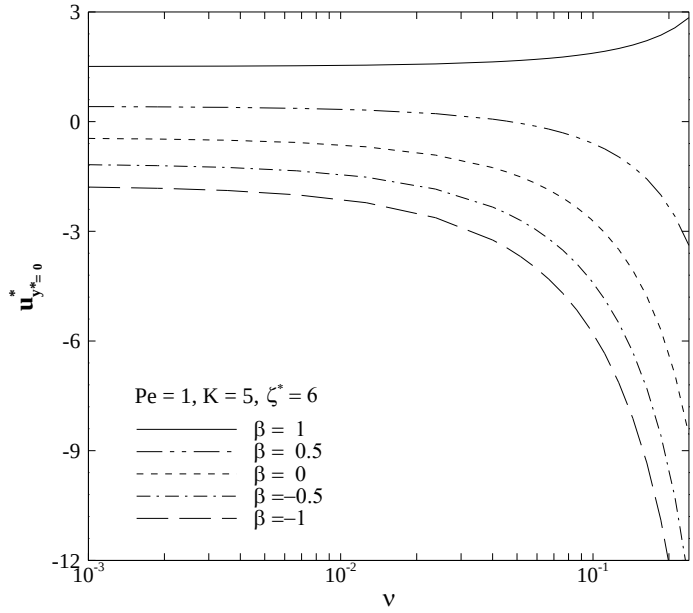

Fig. 5. Velocity at centerline vs. steric factor at different β.

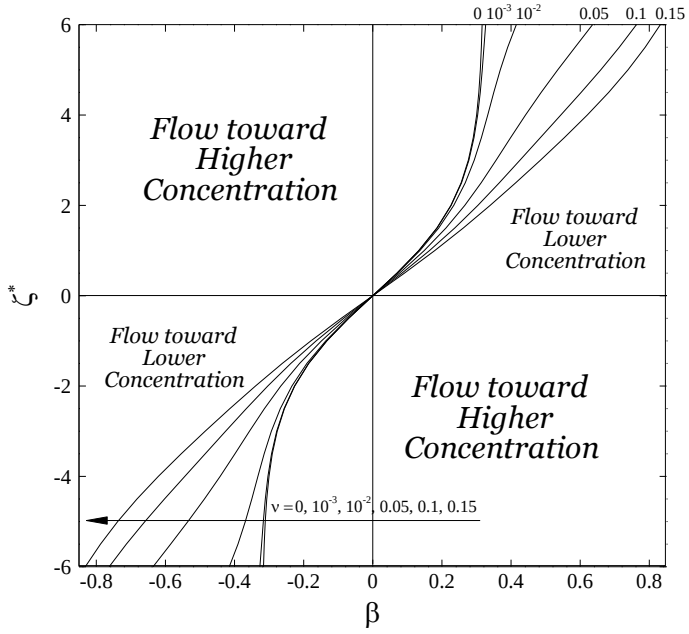

Fig. 6. Flow direction diagram for various ν at K $= 5$ and $Pe = 1$.

We now turn our attention to the most applied graph in the field of DO which is the flow direction diagram. The graph, given in Fig. 6, shows a large degree of synchronization. Each curve divides the graph into four sections that are bounded by the curve and the line $\zeta^* = 0$. Generally, $\zeta^*\beta < 0$ ensures a negative DO velocity whereas the opposite depends on the other flow parameters. As it can be obviously seen, a higher steric factor is accompanied by a diminished chance of flow toward lower concentration. The fact that the flow direction may be changed by making use of for example higher ionic concentrations provides the organ-on-a-chip designers (particularly kidney-on-a-chip where passive mass transport plays an important role) with another mechanism of flow control. Another interesting feature of the graph shown in Fig. 6 is that, unlike the conditions that the ions may be assumed size-less, the flow direction may be changed in the presence of the steric effects by enhancing the surface potential even when $0.4 \leq |\beta|$.

4. CONCLUSIONS

In this research, the ionic size (steric) effects on diffusioosmotic flow through slit microchannels were investigated in order to delineate a closer-to-realistic physics. A theoretical framework was developed under the conditions of a steady and locally developed flow, a small ionic concentration gradient, and a uniform surface potential. It was observed that the steric effects on diffusioosmosis are drastically higher than on other electrokinetic phenomena such as electroosmosis, mainly because of the linkage between the ionic size and the induced electric field. In this respect, the ionic size effects were found to be only negligible when either the steric factor is below 0.001 or the zeta potential is smaller than 25 mV. The steric effects not only change the magnitude of the mean velocity but also can change the flow direction with a tendency to increase the chance of flow toward higher concentration. The interesting thing is

that, again unlike electroosmotic flow, the ionic size effect may lead to higher flow rates for diffusioosmosis; the reason is that the induced electric field may be amplified due to the fact that the stream-wise ionic flux is higher when the ions are assumed to occupy space. Another important finding is that the thin EDL mean velocities are different from those obtained without considering the steric effects which is an evidence for the surprising presence of the ionic size effects even when the EDL is vanishingly small. Last but not least, the deviation from the infinitesimal ionic size results increases by raising the diffusivity of the counterions.

This study was merely dealing with the ionic size effects on the hydrodynamic features of DOF; nevertheless, due to potential applications of diffusioosmosis in both LOCs and drug delivery systems, an understanding of the steric effects on mass transfer capabilities of DOF is highly desirable. The importance of such an analysis is magnified knowing that nothing is reported on the species transport characteristics of DOF. The authors have a plan to provide a thorough mass transfer analysis in the presence of diffusioosmosis in a future work including the effects of finite ionic size on species transport.

ACKNOWLEDGMENT

The research council at Iran University of Science and Technology (IUST) is highly acknowledged for its financial support during the course of this research.

REFERENCES

1 J. H. Masliyah and S. Bhattacharjee, *Electrokinetic and colloid transport phenomena*, John Wiley & Sons, 2006.
2 S. Kandlikar, S. Garimella, D. Li, S. Colin and M. R. King, *Heat transfer and fluid flow in minichannels and microchannels*, Elsevier, 2005.
3 A. Sadeghi, *AlChE J.*, 2015, Accepted.
4 U. Marini Bettolo Marconi, M. Monteferrante and S. Melchionna, *PCCP*, 2014, 16, 25473-25482.
5 S. Tseng, J. P. Hsu, H. M. Lo and L. H. Yeh, *PCCP*, 2013, 15, 11758-11765.
6 C. H. Huang, H. P. Hsu and E. Lee, *PCCP*, 2012, 14, 657-667.
7 H. J. Keh and H. C. Ma, *J. Power Sources*, 2008, 180, 711-718.
8 H. J. Keh and H. C. Ma, *Langmuir*, 2007, 23, 2879-2886.
9 M. S. McAfee, H. Zhang and O. Annunziata, *Langmuir*, 2014, 30, 12210-12219.
10 M. S. McAfee and O. Annunziata, *Langmuir*, 2014, 30, 4916-4923.
11 H. J. Keh and Y. K. Wei, *J. Colloid Interface Sci.*, 2002, 252, 354-364.
12 Y. K. Wei and H. J. Keh, *Colloids Surf., A*, 2003, 222, 301-310.
13 Y. K. Wei and H. J. Keh, *Colloids Surf., A*, 2003, 221, 175-183.
14 J. H. Wu and H. J. Keh, *Colloids Surf., A*, 2003, 212, 27-42.
15 H. J. Keh and H. C. Ma, *Colloids Surf., A*, 2004, 233, 87-95.
16 H. J. Keh and H. C. Ma, *Langmuir*, 2005, 21, 5461-5467.
17 H. C. Ma and H. J. Keh, *Colloids Surf., A*, 2005, 267, 4-15.
18 H. C. Ma and H. J. Keh, *J. Colloid Interface Sci.*, 2006, 298, 476-486.
19 H. C. Ma and H. J. Keh, *J. Colloid Interface Sci.*, 2007, 313, 686-696.
20 L. Y. Hsu and H. J. Keh, *Industrial & Engineering Chemistry Research*, 2008, 48, 2443-2450.
21 H. Keh and L. Hsu, *Microfluid Nanofluid*, 2008, 5, 347-356.
22 H. Keh and L. Hsu, *Microfluid Nanofluid*, 2009, 7, 773-781.
23 H.-F. Huang, *Colloids Surf., A*, 2011, 392, 25-37.

24 Y.-J. Chang, P.-W. Yang and H.-F. Huang, *J. Non-Newtonian Fluid Mech.*, 2013, 194, 32-41.
25 P.-W. Yang, Y.-J. Chang and H.-F. Huang, *Microfluid Nanofluid*, 2013, 1-17.
26 H.-F. Huang and C.-H. Yao, *J. Non-Newtonian Fluid Mech.*, 2014, 206, 1-10.
27 D. C. Prieve, J. L. Anderson, J. P. Ebel and M. E. Lowell, *J. Fluid Mech.*, 1984, 148, 247-269.
28 D. M. Huang, C. Cottin-Bizonne, C. Ybert and L. Bocquet, *Phys. Rev. Lett.*, 2008, 101, 064503.
29 A. Kar, T.-Y. Chiang, I. Ortiz Rivera, A. Sen and D. Velegol, *ACS Nano*, 2015, 9, 746-753.
30 K.-L. Liu, J.-P. Hsu and S. Tseng, *Langmuir*, 2013, 29, 9598-9603.
31 J. J. McDermott, A. Kar, M. Daher, S. Klara, G. Wang, A. Sen and D. Velegol, *Langmuir*, 2012, 28, 15491-15497.
32 H. J. Keh and J. H. Wu, *Langmuir* 2001, 17, 4216-4222.
33 I. Borukhov, D. Andelman and H. Orland, *Phys. Rev. Lett.*, 1997, 79, 435-438.
34 M. S. Kilic, M. Z. Bazant and A. Ajdari, *Phys. Rev. E*, 2007, 75.
35 B. D. Storey, L. R. Edwards, M. S. Kilic and M. Z. Bazant, *Phys. Rev. E*, 2008, 77, 036317.
36 A. S. Khair and T. M. Squires, *J. Fluid Mech.*, 2009, 640, 343-356.
37 A. Garai and S. Chakraborty, *Electrophoresis*, 2010, 31, 843-849.
38 A. Bandopadhyay and S. Chakraborty, *Langmuir*, 2011, 27, 12243-12252.
39 J. Chakraborty, R. Dey and S. Chakraborty, *Phys. Rev. E*, 2012, 86, 061504.
40 R. Dey, T. Ghonge and S. Chakraborty, *Int. J. Heat Mass Transfer*, 2013, 56, 251-262.
41 J. Cervera, P. Ramírez, J. A. Manzanares and S. Mafé, *Microfluid Nanofluid*, 2010, 9, 41-53.
42 A. Bandopadhyay and S. Chakraborty, *Langmuir*, 2012, 28, 17552-17563.
43 A. Bandopadhyay and S. Chakraborty, *Electrophoresis*, 2013, 34, 2193-2198.
44 A. Bandopadhyay, S. S. Hossain and S. Chakraborty, *Langmuir*, 2014, 30, 7251-7258.
45 A. Ahmadian-Yazdi, A. Sadeghi and M. H. Saidi, *J. Colloid Interface Sci.*, 2015, 442, 8–14.
46 A. Ahmadian-Yazdi, A. Sadeghi and M. H. Saidi, *Colloids and Surfaces A*, 2015, Accepted.
47 J. J. Bikerman, *The London, Edinburgh, and Dublin Philosophical Magazine and Journal of Science*, 1942, 33, 384-397.
48 B. Lu and Y. Zhou, *Biophys. J.*, 2011, 100, 2475-2485.
49 A. Shenoy, J. Chakraborty and S. Chakraborty, *Electrophoresis*, 2013, 34, 691-699.